

In Situ Calibration of Colloid Probe Cantilevers in Force Microscopy: Hydrodynamic Drag on a Sphere Approaching a Wall

Vincent S. J. Craig* and Chiara Neto†

Department of Applied Mathematics, Research School of Physical Sciences,
Australian National University, Canberra ACT 0200, Australia

Received March 22, 2001. In Final Form: June 6, 2001

We describe a method for the determination of spring constants for cantilevers used in atomic force microscopes that utilizes the hydrodynamic drag. This simple method is applicable when a spherical colloidal particle has been placed on the tip of the cantilever and requires no extra equipment. The method is applicable to all types of cantilevers and requires that the radius of the colloidal particle and the viscosity of the fluid be known. The deflection of the cantilever under the action of the hydrodynamic drag force in a viscous fluid is measured. As the drag force is known theoretically, the spring constant is determined by application of Hooke's law.

Introduction

Atomic force microscopy (AFM) is frequently employed to determine the interaction forces between a tip and a surface in a variety of fluids. To deduce the measured force from the deflection of the cantilever, the spring constant of the cantilever (k) must be determined accurately. Accurate calibration of the spring constant has been the subject of several publications.^{1–14} As yet, no single method has been widely adopted; rather the method most suitable for a particular set of circumstances is usually employed. This reflects the various limitations and advantages of each technique, which have been discussed widely in the literature.^{9–11,15}

Existing techniques are most suited to the determination of spring constants for bare cantilevers. However, a colloidal particle is often placed on the tip of the cantilever to form a colloid probe, to control the geometry of interaction and the surface properties.^{16–18} The presence

of the particle will change the point of loading on the cantilever and locally alters the stiffness where the particle is attached to the cantilever by glue. The technique we propose here allows the determination of the spring constant of a colloid probe to be made easily and in situ, by measuring the deflection of the cantilever while immersed in a viscous liquid.

Calibration of a spring can be performed in any manner where a deflection can be measured due to a known force. The method described here employs the known hydrodynamic drag force on a sphere approaching a wall perpendicularly. Recently, other methods have been developed using the hydrodynamic drag force to determine the spring constant of AFM cantilevers. Sader et al.¹⁴ have extended earlier work¹³ to enable the determination of spring constants for rectangular cantilevers from the plan view dimensions of the cantilever, the fundamental resonance frequency, and the quality factor in fluid. This method can only be extended to the more commonly used V-shaped cantilevers¹⁹ if they have material properties and thickness identical to an available rectangular cantilever. This usually requires that they are on the same wafer. Maeda et al.²⁰ have measured the drag force and deflection of an AFM cantilever and a scale model (500 times) in order to calibrate AFM cantilevers. Neither of these methods is applicable to colloid probes, as the presence of a particle will greatly change the drag characteristics of the cantilever.

The hydrodynamic drag force F_H , on a sphere of radius b , approaching a wall with velocity U , in a fluid of viscosity η , at a distance h between the center of the sphere and the wall is given exactly by Brenner²¹ for low Reynolds number flow (<1):

$$F_H = 6\pi\eta bU\lambda \quad (1)$$

* To whom correspondence should be addressed. E-mail: vince.craig@anu.edu.au.

† Permanent address: Department of Chemistry, University of Florence, via Gino Capponi 9, 50121 Firenze, Italy.

(1) Cleveland, J. P.; Manne, S.; Bocek, D.; Hansma, P. K. *Rev. Sci. Instrum.* **1993**, *64*, 403–405.

(2) Hutter, J. L.; Bechhoefer, J. *Rev. Sci. Instrum.* **1993**, *64*, 1868–1873.

(3) Sader, J. E.; White, L. *J. Appl. Phys.* **1993**, *74*, 1–9.

(4) Senden, T. J.; Ducker, W. A. *Langmuir* **1994**, *10*, 1003–1004.

(5) Rabinovich, Y. I.; Yoon, R. H. *Langmuir* **1994**, *10*, 1903–1909.

(6) Chen, G. Y.; Warmack, R. J.; Thundat, T.; Allison, D. P.; Huang, A. *Rev. Sci. Instrum.* **1994**, *65*, 2532–2537.

(7) Neumeister, J. M.; Ducker, W. A. *Rev. Sci. Instrum.* **1994**, *65*, 2527–2531.

(8) Butt, H.-J.; Jaschke, M. *Nanotechnology* **1995**, *6*, 1–7.

(9) Sader, J. E.; Larson, I.; Mulvaney, P.; White, L. R. *Rev. Sci. Instrum.* **1995**, *66*, 3789–3798.

(10) Gibson, C. T.; Watson, G. S.; Myrha, S. *Nanotechnology* **1996**, *7*, 259–262.

(11) Torii, A.; Sasaki, M.; Hane, K.; Okuma, S. *Meas. Sci. Technol.* **1996**, *7*, 179–184.

(12) Walters, D. A.; Cleveland, J. P.; Thomson, N. H.; Hansma, P. K.; Wendman, M. A.; Gurley, G.; Elings, V. *Rev. Sci. Instrum.* **1996**, *67*, 3583–3590.

(13) Sader, J. E. *J. Appl. Phys.* **1998**, *84*, 64–76.

(14) Sader, J. E.; Chon, J. W. M.; Mulvaney, P. *Rev. Sci. Instrum.* **1999**, *70*, 3967–3969.

(15) Useful discussions on the relative merits of different methods of calibrating spring constants and the errors involved can be found by searching at <http://www.di.com/search/query.asp> using "spring constant".

(16) Ducker, W. A.; Senden, T. J.; Pashley, R. M. *Nature* **1991**, *353*, 239–241.

(17) Ducker, W. A.; Senden, T. J.; Pashley, R. M. *Langmuir* **1992**, *8*, 1831–1836.

(18) Butt, H.-J. *Biophys. J.* **1991**, *60*, 1438–1444.

(19) "V"-shaped cantilevers are often preferred for force measurement as twisting motions are minimized by the high torsional stiffness conferred by this geometry.

(20) Maeda, N.; Senden, T. J. *Langmuir* **2000**, *16*, 9282–9286.

(21) Brenner, H. *Chem. Eng. Sci.* **1961**, *16*, 242–251.

where

$$\lambda = \frac{4}{3} \sinh \alpha \sum_{n=1}^{\infty} \frac{n(n+1)}{(2n-1)(2n+3)} \left[\frac{2 \sinh (2n+1)\alpha + (2n+1) \sinh 2\alpha}{4 \sinh^2 (n+(1/2))\alpha - (2n+1)^2 \sinh 2\alpha} - 1 \right] \quad (2)$$

and

$$\alpha = \cosh^{-1} \left(\frac{h}{b} \right) \quad (3)$$

The theory of Brenner has been experimentally verified using both macroscopic and microscopic spheres.^{22–24} When the distance between the surface of the sphere and the wall, a (where $a = h - b$), is small compared to the radius of the sphere, b , Brenner's equation can be accurately approximated by the following equation:^{22,25,26}

$$F_H = 6\pi\eta b U \frac{b}{a} \quad (4)$$

Equation 4 is used here to calculate the hydrodynamic drag force on the sphere and consequently derive the spring constant of the AFM cantilever to which the sphere is attached. In Figure 1 the hydrodynamic forces given by eqs 1 and 4 are compared for parameter values typically encountered in the experiments reported here. At very small separations the theories are in very good agreement. As the separation increases, the approximation is more in error. At a separation of 1750 nm the percent error due to the approximate theory is 16%, but the absolute error is only 0.02 nN. This error is smaller than the noise in the experimental data and therefore can be ignored.

Methods

To investigate the hydrodynamic force exerted on a sphere approaching a flat in a fluid, we placed a smooth sphere at the end of the AFM cantilever (see Figure 2). Standard silicon nitride V-shaped cantilevers of length 200 μm with a leg width 40 μm (long, fat) were used (Digital Instruments, Santa Barbara, CA). Silica spheres of radius approximately 10 μm were sourced from Duke Scientific (roughness 0.11 nm RMS over 100 \times 100 nm^2). A freshly cleaved sheet of muscovite mica was usually used as a flat substrate. Surfaces were cleaned using a radio frequency generated, low-temperature water plasma²⁷ (20 W for 30 s). A Nanoscope (III) Multimode AFM (Digital Instruments) was used for all imaging and force measurements.

Aqueous solutions of analytical grade sucrose (BDH) were used at various concentrations to produce solutions with a range of viscosity between 5 and 80 mPa s (note: the viscosity of water at 20 °C is 1 mPa s). The viscosity as a function of weight percent of sucrose was determined from tabulated values.²⁸ The room temperature was 20 \pm 0.1 °C during experiments. Under the experimental conditions employed here, the Reynolds number was always less than 10⁻⁵. We used different surfaces in order to test the general validity of our results. For most experiments

(22) Mackay, G. D. M.; Mason, S. G. *J. Colloid Sci.* **1961**, *16*, 632–635.

(23) Mackay, G. D. M.; Suzuki, M.; Mason, S. G. *J. Colloid Sci.* **1963**, *18*, 103–104.

(24) Pagac, E. S.; Tilton, R. D.; Priev, D. C. *Chem. Eng. Commun.* **1996**, *148–150*, 105–122.

(25) Chan, D. Y. C.; Horn, R. G. *J. Chem. Phys.* **1985**, *83*, 5311–5324.

(26) Horn, R. G.; Vinogradova, O. I.; Mackay, M. E.; Phan-Thien, N. *J. Chem. Phys.* **2000**, *112*, 6424–6443.

(27) <http://www.rspphysse.anu.edu.au/appmaths/plasma.html>.

(28) *Handbook of Physics and Chemistry*, 80th ed.; Baysinger, G., Craig, N. C., Goldberg, R. N., Koetzle, T. F., Kuchitsu, K., Lin, C. C., Smith, A. L., Frederikse, H. P. R., Lide, D. R., Eds.; CRC Press: Boca Raton, 1999–2000.

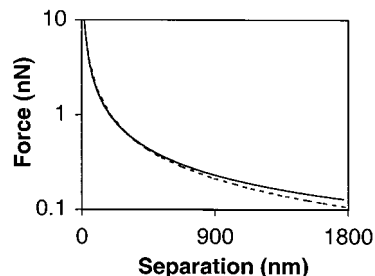


Figure 1. Comparison of the approximate theory (Taylor equation) (dotted line) with the exact theory due to Brenner presented in eq 1 (solid line) for the hydrodynamic drag force on a sphere moving perpendicular to a solid wall as a function of separation. The semilog scale is chosen to highlight the error of the approximate theory at large separations. Both calculations are for a drive rate of 2396 nm/s, a viscosity of 38.9 mPa s, and a sphere radius of 10.4 μm . These are typical values used in the experiments described below.

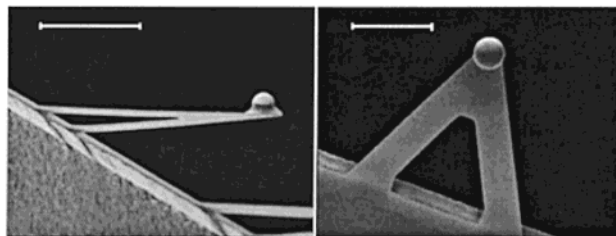


Figure 2. Scanning electron microscope images of a V-shaped cantilever spring (Digital Instruments) with a silica sphere attached to the tip. The image on the left is a side view indicating the thickness of the spring and the glue used to hold the sphere in position. The addition of the glue will alter the stiffness of the spring. The image on the right shows the sphere as it would appear from the flat surface. The point of loading is shifted upon placement of the sphere resulting in a change in spring constant. Both the scale bars are 50 μm .

both the sphere and the mica were gold coated (15.1 ± 0.2 nm) using a layer of titanium (7.7 ± 0.2 nm) to promote adhesion. The RMS roughness of the gold surfaces was determined by AFM to be 0.56 nm over 1000 \times 1000 nm^2 (note that the contact area is around 20 \times 20 nm^2). In some experiments (cantilevers B, D, E, and F in Table 3) the gold surfaces were treated with mixtures of 10 mM 11-mercapto-1-undecanol and 10 mM 1-dodecanethiol in ethanol to produce a self-assembled monolayer (SAM). A bare silica sphere and a silicon surface (cantilever C, Table 3) and a gold-coated sphere and a silica surface (cantilever A, Table 3) were also used.

The cantilevers calibrated with the proposed hydrodynamic method were sourced from two separate wafers (W1 and W2). A calibration of a number of bare cantilevers (no colloid probe attached) from the same wafers was performed for comparison using the Cleveland method¹ corrected for off-end loading.⁹ Tungsten microspheres (BioForce Lab., Inc.) were attached to the cantilevers with Epicote glue (Shell), and the spring constant was determined from the frequency shift of the loaded cantilevers. When possible, the same cantilevers employed in hydrodynamics experiments (with the colloid probe still attached) were subsequently calibrated with the Cleveland method to permit a direct comparison of the two methods. The diameter of the tungsten spheres and of the colloid spheres was measured to within ± 0.1 μm with a Cambridge S360 scanning electron microscope (SEM).

The AFM makes use of a light lever to detect the deflection of a fine cantilever as a flat surface is moved perpendicularly toward it, using a piezoelectric transducer. The ramp rate of the flat surface can be accurately controlled and varied over 3 orders of magnitude. For each solution studied, data was captured over a wide range of approach velocities. The deflection versus piezo travel data was converted to deflection (or force) versus separation in the usual manner.¹⁷ The sensitivity of the light lever (commonly referred to as compliance) is determined by the change in signal at the diode due to the deflection of the cantilever when the

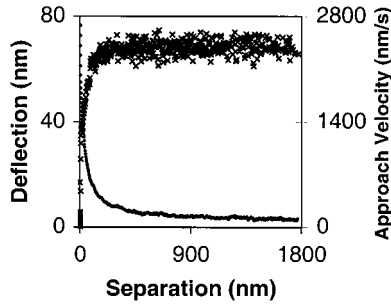


Figure 3. Measured spring deflection (circles, left ordinate axis) and approach velocity (crosses, right ordinate axis) as a function of surface separation. The flat surface is being driven at a velocity of 2396 nm/s toward a sphere of radius 10.4 μm in a solution of viscosity 38.9 mPa s. As the surface separation is decreased, the magnitude of the hydrodynamic force and hence the spring deflection increase. As the spring is deflected away from the flat surface, the approach velocity of the sphere and the flat is decreased. The plotted approach velocity is derived from the sum of the ramp velocity (positive) and the velocity of the cantilever deflection (negative).

substrate and sphere are in contact. At large approach velocities it is difficult to determine the compliance accurately as the repulsive forces are large. Therefore, when necessary the compliance was determined from data obtained using low approach velocities.

The velocity at which the substrate moves is accurately controlled by the piezoelectric transducer, but it is not equivalent to the approach velocity of the surfaces at all times. When the hydrodynamic repulsive force on the sphere becomes significant, the spring will be deflected away from the substrate.²⁹ This results in a reduced relative velocity of the surfaces. For each data point, the actual approach velocity (U) can be calculated by summing the velocity at which the flat surface is driven (positive values) and the velocity of the tip deflection (negative values for a repulsive force). The adjustment is significant when the repulsive force rises steeply with distance. The measured spring deflection (x) and calculated approach velocity (U) for a typical measurement are shown in Figure 3. In this case, at a separation of 10 nm the approach velocity has fallen to $\sim 50\%$ of the piezo drive rate.

From Hooke's law ($F = kx$) and eq 4 the following relation holds:

$$6\pi\eta b^2 \frac{1}{a} = kx_{\text{norm}} \quad (5)$$

where x_{norm} is the normalized spring deflection, obtained by dividing the measured spring deflection (x) by the actual approach velocity (U). A plot of the normalized deflection (x_{norm}) versus the inverse of the separation ($1/a$) gives a straight line of slope m , which is used to determine the spring constant:

$$k = 6\pi\eta b^2 / m \quad (6)$$

As the solution viscosity (η) and sphere radius (b) can be determined independently, the only unknown is the spring constant, k . Experimental data are used when the R^2 obtained from a linear regression is greater than 0.99. A spreadsheet file that performs all the necessary calculations for force scaling and spring calibration is available from the authors.

The measured drag force consists of the sum of the drag force on the cantilever spring and the drag force on the sphere. At large separations the cantilever due to its size and shape dominates the drag force. As the surface separation is reduced, the drag force on the cantilever increases only slightly as the cantilever is always at a distance greater than the sphere diameter ($\sim 20 \mu\text{m}$) away from the flat surface, but the drag force on the sphere increases rapidly. When the surface separation a is smaller than the sphere radius b , the measured drag force is

(29) The effect of the spring deflection on the surface separation is taken into account during the normal procedure for converting deflection curves to force curves.¹⁷

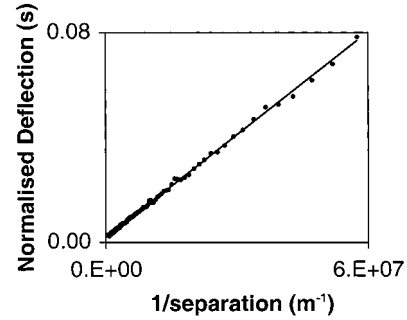


Figure 4. Normalized spring deflection (circles) and its linear regression (line). The normalized deflection is the spring deflection divided by the approach velocity (hence its units are seconds). The R^2 obtained from the linear regression is 0.9988. The experiment was conducted in a sucrose solution of viscosity 80.3 mPa s, and the approach velocity was 1472.4 nm/s. The spring constant was determined to be $k = 0.113 \text{ N/m}$.

Table 1. Results of Calibration on a V-Shaped Cantilever (F, Wafer 2) with the Proposed Hydrodynamic Method

driving rate (nm/s)	viscosity (mPa s)	spring constant k (N/m)
1 472.4	80.3	0.111
2 396	27.0	0.102
2 816.8	19.2	0.110
4 048	80.3	0.114
4 800	27.0	0.103
8 100	38.9	0.118
9 968	80.3	0.117
11 780	19.2	0.112
11 780	80.3	0.111
16 196	19.2	0.118
16 196	38.9	0.119
21 596	19.2	0.118
21 596	38.9	0.121

Average $k \pm \sigma = 0.113 \pm 0.06$

dominated by the drag on the sphere. In AFM force measurements it is necessary that the zero force (or baseline) is determined. Usually the cantilever deflection at large separations is constant because no surface force is acting on the cantilever. This situation is therefore defined as zero force. In viscous solutions at high approach velocities the hydrodynamic force is significant even at large separations. This prevents the determination of the zero of force in the usual manner. When presenting force versus separation data, this has been overcome by adjusting the data such that the measured data at the largest separation ($\sim 2000 \text{ nm}$) coincides with the theoretical drag force on the sphere. This adjustment has no effect on the slope of the data and therefore no effect on the calculated spring constant.

Results and Discussion

The normalized deflection versus the inverse of separation is shown in Figure 4 for surface separations between 1800 and 15 nm. As discussed before, a linear relationship is observed. A linear regression of the data is obtained and the slope of the line is determined. Application of eq 5 yields the spring constant. It is advisable to exclude data points obtained at very small separations, as they may be significantly affected by the presence of surface forces and data points obtained at large separations, as they are affected by the initial rapid acceleration of the piezo. Deflection versus separation measurements for a single colloid probe are typically made in a variety of solutions at different approach rates. Each measurement yields an independent measure of the spring constant and can therefore be used to increase the accuracy of the determination. Typical results are presented in Table 1.

The results presented in Figure 5 are for the same system as in Figure 4, but a larger drive rate is employed.

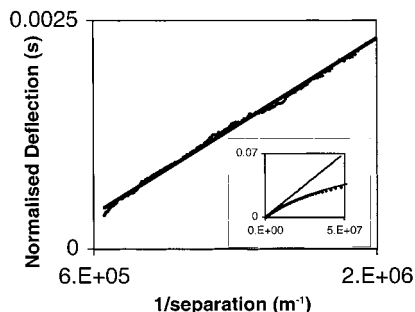


Figure 5. Normalized spring deflection (circles) and its linear regression (line). The R^2 obtained from the linear regression is 0.9967. In the inset (units are the same as in the main figure) the experimental data (circles) is presented in full scale together with the Brenner theory (straight line) and the hydrodynamic force allowing for slip,^{29,30} using a slip length of 13 nm (curved line). All three curves agree closely at large separations. At separations less than 500 nm (inset) the experimental data can only be fit by allowing for a partial slip boundary condition. The different behavior of the no-slip and the slip theories at small separations is clearly shown in the inset. A spring constant of 0.113 N/m was obtained from the linear data at large separations. The experiment was conducted in a sucrose solution of viscosity 80.3 mPa s, and the approach velocity was 9968 nm/s.

At separations greater than 500 nm a linear relationship is observed. However, at smaller separations significant deviations from linearity are observed (inset). This is attributed to partial boundary slip³⁰ and therefore cannot be modeled with eqs 1 and 4, which are formulated using the no-slip boundary condition. Without knowing the precise nature of the fluid slip at the fluid–solid interface, the data in this region cannot be used to determine the spring constant. The hydrodynamic force and boundary slip have been addressed in detail in another paper.³¹ It was found that boundary slip increases as both the approach velocity and the viscosity of the solution are increased. For this reason a fluid of viscosity 50 mPa s or less is preferable for spring constant determination and the fit should be made at separations of greater than 200 nm. In any case, the measured deflection at small separations should not be used to determine the spring constant as this region may be affected by surface forces and surface roughness. The inset in Figure 5 highlights the different behaviors of the no-slip (straight line) and the slip (curved line) theories at small separations. The spring constant may still be obtained from the data at large separations, in the range where the normalized deflection versus 1/separation data is linear. When these guidelines are followed, the spring constants determined in the presence and absence of boundary slip agree. We note that boundary slip can be avoided by appropriate choice of ramp velocity and fluid viscosity. Experimental force versus separation data are presented in the conventional manner in Figure 6, using a spring constant value that has been determined as described above. Agreement is found between the experimental data and the theoretical hydrodynamic drag force over all separations.

Spring constants determined using the Cleveland method¹ are reported in Table 2. The scatter in the calculated values is high even within cantilevers from the same wafer. The spring constant of a cantilever often varies with its location within the wafer. This is attributed to changes in spring thickness and material properties that occur within a wafer during the manufacturing process.

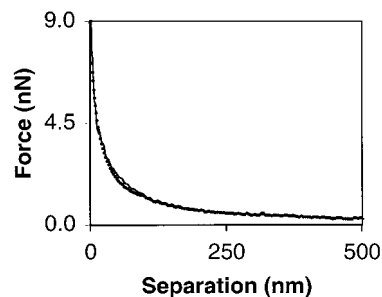


Figure 6. Comparison of the measured hydrodynamic force (circles) with eq 4 (line). A spring constant of 0.14 N/m has been used. The experiment was conducted with a gold-coated colloid probe and a silicon surface in sucrose solution of viscosity 32.8 mPa s. The colloid probe radius was 8.86 μm . The approach velocity was 2816.8 nm/s.

Table 2. Results of Cantilever Calibration with the Cleveland Method¹ Corrected for Off-End Loading^{9 a}

wafer	cantilever no.	spring constant k (N/m)
W1	3	0.068
W1	5	0.090
W1	6	0.043
W1	8	0.043
Average $k \pm \sigma = 0.061 \pm 0.02$		
W2	2	0.11
W2	3	0.13
W2	4	0.098
W2	5	0.09
W2	6	0.10
W2	7	0.050
W2	8	0.20
W2	9	0.17
W2	10	0.19
W2	11	0.12
W2	12	0.12
W2	13	0.10
W2	14	0.054
W2	15	0.42
W2	16	0.14

Average $k \pm \sigma = 0.14 \pm 0.09$

^a The cantilevers (Digital Instruments) presented here are 200 μm in length and 40 μm in leg width, all from two wafers (W1 and W2). The nominal value for the spring constants given by the manufacturer is 0.01–0.6 N/m. The tungsten particles of radius 6–8 μm (BioForce Lab., Inc.) were assumed to have the bulk density of tungsten (19 300 kg m^{-3}).

Some wafers will be more uniform than others. Due to this variation it is preferable to calculate the spring constant of the cantilever actually used in a force experiment. One advantage of the method we propose is that the spring constant of the actual spring used for force measurements can be determined after an experiment, in situ. This avoids the assumption that springs within a wafer are identical.

Spring constants determined using the proposed hydrodynamic method are reported in Table 3. The spring constant of cantilevers from wafer W2 determined with the Cleveland method (see Table 2) agree with the spring constant values obtained for cantilevers A, B, and C using the hydrodynamic method. On three cantilevers (A, B, and F) the two calibration methods were compared directly by applying the Cleveland method after the hydrodynamic experiments. The agreement for A and B is good but approximate for F. Two tungsten spheres were inadvertently placed on this cantilever at different positions. It is likely that the correction for off-end loading in this case is in error and has led to an error in the spring constant determined by the Cleveland method. Errors in spring constant due to the placement of the colloid probe are

(30) Vinogradova, O. I. *Langmuir* **1998**, *14*, 2827–2837.

(31) Craig, V. S. J.; Neto, C.; Williams, D. R. M. Submitted for publication in *Phys. Rev. Lett.*

Table 3. Results of Cantilever Calibration with the Proposed Hydrodynamic Method and with the Cleveland Method¹ Corrected for Off-End Loading^{9 a}

wafer	cantilever	spring constant k (N/m)	
		hydrodynamic method	Cleveland method
W2	A	0.140	0.15
W2	B	0.140	0.12
W2	C	0.155	N/A
W2	D	0.190	N/A
W1	E	0.124	N/A
W1	F	0.113	0.14 ^b

^a The cantilevers (Digital Instruments) presented here are 200 μm in length and 40 μm in leg width. The spring constants for the different cantilevers were derived from hydrodynamic experiments using different surfaces: (A) gold-coated colloid probe and silicon surface; (C) silica colloid probe and silicon surface; (B, D, E, and F) both surfaces gold coated covered with a mixed SAM (see Methods section). ^b Two tungsten spheres were inadvertently attached to this cantilever. This complicates the correction for off-end loading and hence could introduce a high error in the spring constant.

excluded by the hydrodynamic method described here, as the spring constant of the cantilever is measured after attachment of the particle.

A source of error in AFM force measurements is the reflection and scattering of the laser beam from the substrate onto the photodiode creating interference with the light reflected from the cantilever.³² This is manifest as a sinusoidal wave on the baseline of force measurements with a wavelength of $\sim\lambda/2n$, where λ is the wavelength of the laser light and n is the refractive index of the fluid. The effect of this error can be minimized by choosing a system in which the forces are large. Hence solutions of viscosity much greater than water have been used in this study to increase the drag force on the sphere. Low-viscosity solutions can be employed when the errors due to optical interference are small as is likely in many systems. Aqueous salt solutions are preferable to pure water as the range of force due to the double layer is compressed.

The Duke Scientific spheres are extremely smooth, but their roughness is slightly increased by gold coating. The spring constants obtained with the different spheres are very similar. Any change in the hydrodynamic drag force due to roughness will be manifest at small separations, whereas the force at small separations is not used to determine the spring constant as it may be influenced by surface forces or boundary slip. Hence small-scale roughness of the sphere does not influence the spring constant determination.

There are errors in the measurement of the radius of the colloid particle and in the viscosity of the fluid that

will affect the accuracy of this method. The error in the radius determination for 10 μm spheres is typically $\sim 0.5\%$ if measured by SEM (the error can be substantially larger for smaller spheres: 2% for a 3 μm sphere). The square of the radius is required to calculate the hydrodynamic force (see eq 4); therefore the error is $\sim 1.0\%$ (4% for a 3 μm sphere). Techniques requiring the placement of a known mass on the cantilever usually require that the mass is determined from its volume; thus the cube of the radius is required and the error is $\sim 1.5\%$ (6% for a 3 μm sphere). Hence, the error introduced by the radius measurement is less for the hydrodynamic method. Further, experimental force curves are usually normalized by the radius (F/R) in order to allow comparison with theory. Using the hydrodynamic method, the sphere (and therefore radius) used for the spring constant determination is the same as that used for normalization; thus the error in the radius will have a linear effect on the error in F/R . The viscosity of a fluid can be determined very accurately provided the temperature of the fluid is controlled. Thus the degree of temperature control will determine the error in the viscosity. With good temperature control (± 0.1 °C) the error in viscosity will be $< 1\%$. Errors associated with force measurements using the AFM such as piezo calibration and determining the compliance also apply to the determination of the spring constant by this method. These errors are more difficult to quantify.

Brenner²¹ has also derived an exact solution for a sphere moving parallel to a wall for low Reynolds number flow. This should provide a means for determining the lateral or twisting spring constant of a cantilever, which is important for quantitative determination of frictional forces. Work on this is continuing. In summary, a technique specifically aimed at determining the spring constants of cantilevers bearing colloid probes has been developed. The technique is easy to employ, requires no extra equipment, and has accuracy comparable to that of other methods.

Acknowledgment. We thank Graeme Jameson for helpful discussions on hydrodynamics and for bringing to our attention the work of Brenner. Shannon Notley contributed to efforts to determine spring constants hydrodynamically using an oscillating substrate. Detailed discussions with Phil Attard on the techniques and possible sources of error are appreciated. David Williams has been of great assistance in the analysis of slip behavior, and discussions with Tim Senden and Nobuo Maeda were most helpful. V.S.J.C. gratefully acknowledges the support of an Australian Research Council funded postdoctoral fellowship. C.N. acknowledges the Italian Ministry for Scientific Research (MURST) and CSGI.

LA010424M

(32) Janschke, M.; Butt, H.-J. *Rev. Sci. Instrum.* **1995**, *66*, 1258–1259.